CHINESE JOURNAL OF CHEMICAL PHYSICS VOLUME 30, NUMBER 6 DECEMBER 27, 2017

ARTICLE

Structural and Electronic Properties of $Co_nC_3{}^{-/0}$ and $Co_nC_4{}^{-/0}$ (n=1−4) Clusters: Mass-Selected Anion Photoelectron Spectroscopy and Density Functional Theory Calculations[†]

Xi-ling Xu[a,c], Jin-yun Yuan[b], Bin Yang[a,c], Hong-guang Xu[a,c], Wei-jun Zheng[a,c]*

a. Beijing National Laboratory for Molecular Sciences (BNLMS), State Key Laboratory of Molecular Reaction Dynamics, Institute of Chemistry, Chinese Academy of Sciences, Beijing 100190, China
b. School of Material and Chemical Engineering, Zhengzhou University of Light Industry, Zhengzhou 450002, China
c. University of Chinese Academy of Sciences, Beijing 100049, China

(Dated: Received on October 30, 2017; Accepted on December 4, 2017)

We investigated the structural evolution and electronic properties of $Co_nC_3{}^{-/0}$ and $Co_nC_4{}^{-/0}$ (n=1−4) clusters by using mass-selected photoelectron spectroscopy and density functional theory calculations. The adiabatic and vertical detachment energies of $Co_{1-4}C_3{}^-$ and $Co_{1-4}C_4{}^-$ were obtained from their photoelectron spectra. By comparing the theoretical results with the experimental data, the global minimum structures were determined. The results indicate that the carbon atoms of $Co_nC_3{}^{-/0}$ and $Co_nC_4{}^{-/0}$ (n=1−4) are separated from each other gradually with increasing number of cobalt atoms but a C_2 unit still remains at n=4. It is interesting that the $Co_2C_3{}^-$ and $Co_2C_4{}^-$ anions have planar structures whereas the neutral Co_2C_3 and Co_2C_4 have linear structures with the Co atoms at two ends. The $Co_3C_3{}^-$ anion has a planar structure with a Co_2C_2 four-membered ring and a Co_3C four-membered ring sharing a Co−Co bond, while the neutral Co_3C_3 is a three-dimensional structure with a C_2 unit and a C atom connecting to two faces of the Co_3 triangle.

Key words: Photoelectron spectroscopy, Transition metal carbide, Structural evolution, Density functional calculations

I. INTRODUCTION

Transition-metal carbides possess unique physical and chemical properties, such as high melting point, extreme hardness, high electrical conductivity, and high thermal conductivity. They have many applications in cutting tools and hard-coating materials. It has been suggested that some early transition-metal carbides exhibited unique and intriguing Pt-like catalytic properties [1], especially in the reactions involving C−H bond activation [2, 3]. Transition-metal atoms not only can be trapped inside fullerene cages to form endohedral metallofullerenes [4, 5], but also can be incorporated into a carbon cage and thus become a part of the cage [6]. Metallo-carbohedrenes (met-cars) in the form of M_8C_{12} have very symmetric cage structures with the metal atoms incorporated in the cage [7−10]. Recently, a series of two-dimensional metal carbides known as MXenes were synthesized using early transition metals and were proposed to be promising electrode materials for Li-ion batteries, non-Li ion batteries, and supercapacitor [11−13]. It has been reported that the late transition metals such as Fe, Co, and Ni or their alloys can catalyze the growth of single-walled carbon nanotubes [14−17].

The previous studies indicate that the transition-metal carbide clusters show very diverse structures. The most stable structures of $V_4C_4{}^-$ [18] and Ti_4C_4 [19] were suggested to be T_d symmetric cubic structure with the C atoms isolated by the metal atoms. Wang and coworkers investigated the structures and electronic properties of 3d mono-metal carbides, $TiC_n{}^-$ (n=2−5) [20] and $FeC_n{}^-$ (n=2−4) [21, 22], using anion photoelectron spectroscopy and density functional study. They found that $TiC_n{}^-$ (n=2−5) and $FeC_3{}^-$ have ring structures, while $FeC_4{}^-$ has a linear structure with the Fe atom bonded at one end. They also studied a series of 4d mono-niobium carbide clusters, $NbC_n{}^-$ (n=2−7), using anion photoelectron spectroscopy and found a cyclic to linear structural transition from $NbC_3{}^-$ to $NbC_4{}^-$ [23]. The investigation of Castleman and coworkers showed that $Nb_2C_n{}^-$ (n=4−9) clusters have linear isomers for odd-numbered clusters, along with planar rings and 3D structures [24].

[†] Part of the special issue for "the Chinese Chemical Society's 15th National Chemical Dynamics Symposium".

*Author to whom correspondence should be addressed. E-mail: zhengwj@iccas.ac.cn, Tel.: +86-10-62635054, FAX: +86-10-62563167

DOI:10.1063/1674-0068/30/cjcp1710197

Owing to the importance of CoC in carbon-rich circumstellar shells and the applications of cobalt carbides in the field of catalyst and material science, there were many theoretical and experimental studies on cobalt carbide clusters. Diatomic $CoC^{+/0}$ have been extensively investigated by experiments [25–30] and theoretical calculations [31–34]. The structures of $CoC_{1-8}{}^{+/-/0}$ [35–37] and CoC_{9-15} [38] were investigated by density functional theory. The structures of cobalt carbide clusters containing two or multiple cobalt atoms, such as Co_2C_{1-6} [37] and $Co_{1-5}C_2$ [39], were also investigated by theoretical calculations. The electronic and structural properties of $CoC_{2,3}{}^-$ [40, 41], $Co_2C_{2,3}{}^-$ [42], and $Co_{1-5}C_2$ [43] were studied with anion photoelectron spectroscopy. Furthermore, the structures of cobalt acetylide species $Co_nC_2H_2{}^-$ (n=1−3) [44] and $Co_nC_2H^-$ (n=1−5) [45] were investigated with mass-selected anion photoelectron spectroscopy and density functional theory calculations. The formation of carbide, especially Co_2C, is often referred to as a sign of deactivation and the active components on cobalt catalysts are usually considered to remain in metallic states during Fischer-Tropsch synthesis [46]. Harris *et al.* have reported the cobalt carbide nanoparticles (Co_3C and Co_2C phases) with a coercivity over 3 kOe at room temperature, fabricated by a direct chemical synthesis method [47]. Gao *et al.* found that orthorhombic fullerene-like Co_3C nanoparticles displayed excellent electrochemical hydrogen storage capacity at room temperature and ambient pressure, which can be prepared by mechanical alloying method [48].

In this work, to extend the range of cobalt carbide cluster stoichiometries and give insight into the structural evolution and electronic properties of cobalt carbides, we investigated $Co_nC_3{}^{-/0}$ and $Co_nC_4{}^{-/0}$ (n=1−4) clusters with mass-selected anion photoelectron spectroscopy and density functional calculations.

II. EXPERIMENTAL AND THEORETICAL METHODS

The experiments were performed using a home-built apparatus consisting of a time-of-flight (TOF) mass spectrometer and a magnetic-bottle photoelectron spectrometer, which has been described previously [49]. Briefly, the $Co_nC_3{}^-$ and $Co_nC_4{}^-$ (n=1−4) cluster anions were generated in a laser vaporization source by laser ablation of a rotating and translating cobalt-carbon mixture disk target (13 mm diameter, Co:C mole ratio 5:1) with the second harmonic light (532 nm) of a Nd:YAG laser (Continuum Surelite II-10), while helium gas with ∼4 atm backing pressure was allowed to expand through a pulsed valve (General Valve Series 9) over the target for cooling the formed clusters. The cluster anions were mass-analyzed by the TOF mass spectrometer. The $Co_nC_3{}^-$ and $Co_nC_4{}^-$ (n=1−4) clusters were each mass-selected and decelerated before being photodetached using the second (532 nm@2.331 eV) or fourth (266 nm@4.661 eV) harmonic lights of another Nd:YAG laser. The photodetached electrons were energy-analyzed by the magnetic-bottle photoelectron spectrometer. The photoelectron spectra were calibrated using the spectra of Cu^- and Au^- taken under similar conditions. The energy resolution of the photoelectron spectrometer was approximately 40 meV for the electrons of 1 eV kinetic energy.

The swarm-intelligence-based CALYPSO structure prediction software [50] was utilized to search the possible structures for $Co_nC_3{}^{-/0}$ and $Co_nC_4{}^{-/0}$ (n=1−4) clusters. The CALYPSO is an efficient structure prediction method, which requires only chemical compositions for a given cluster to predict stable or metastable structures at given external conditions. The structures obtained using the CALYPSO were further optimized using density functional theory with the Becke's exchange [51] and Perdew-Wang correlation functional (BPW91) [52] and 6-311+G(d) basis set as implemented in the Gaussian 09 program package [53]. The BPW91 functional has been shown to be suitable for transition-metal-containing clusters in previous reports [18, 43, 54]. To confirm the reliability of 6-311+G(d) basis set, we also calculated the relative energies and vertical detachment energies (VDEs) of the small size $Co_{1,2}C_3{}^-$ clusters using the aug-cc-pVTZ [55] basis set with the same functional. The results obtained from the 6-311+G(d) basis set are very close to those from the aug-cc-pVTZ basis set (See Table S1 in the supplementary materials). Because the aug-cc-pVTZ basis set is more expensive than the 6-311+G(d) basis set, here we chose the BPW91/6-311+G(d) method for the calculations in this work. We have considered all possible spin multiplicities during the calculations. All the geometry optimizations were conducted without any symmetry constraint. Harmonic vibrational frequencies were calculated to make sure that the optimized structures correspond to true local minima. The zero-point vibrational energy corrections were included for the relative energies of isomers. The theoretical VDE was calculated as the energy difference between the neutral and anion at the geometry of the anionic species. The theoretical adiabatic detachment energy (ADE) was calculated as the energy difference between the neutral and anion with the neutral relaxed to the nearest local minimum using the geometry of the corresponding anion as initial structure. The atomic dipole moment corrected Hirshfeld population (ADCH) analysis [56] of $Co_nC_3{}^{-/0}$ and $Co_nC_4{}^{-/0}$ (n=1−4) was performed with the Multiwfn program [57]. The ADCH charge analysis is an improved version of Hirshfeld charge analysis [58]. The Wiberg bond order analyses of $Co_nC_3{}^{-/0}$ and $Co_nC_4{}^{-/0}$ (n=1−4) were conducted with natural bond orbital (NBO) version 3.1 program [59] implemented in the Gaussian 09 package.

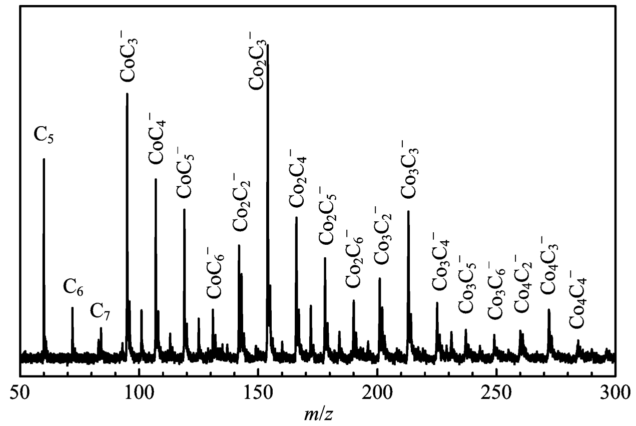

FIG. 1 A typical mass spectrum of $Co_nC_m^-$ anions generated in our experiments. The highest intensity series is $Co_nC_3^-$ (n=1−4) and the second one is $Co_nC_4^-$ (n=1−4).

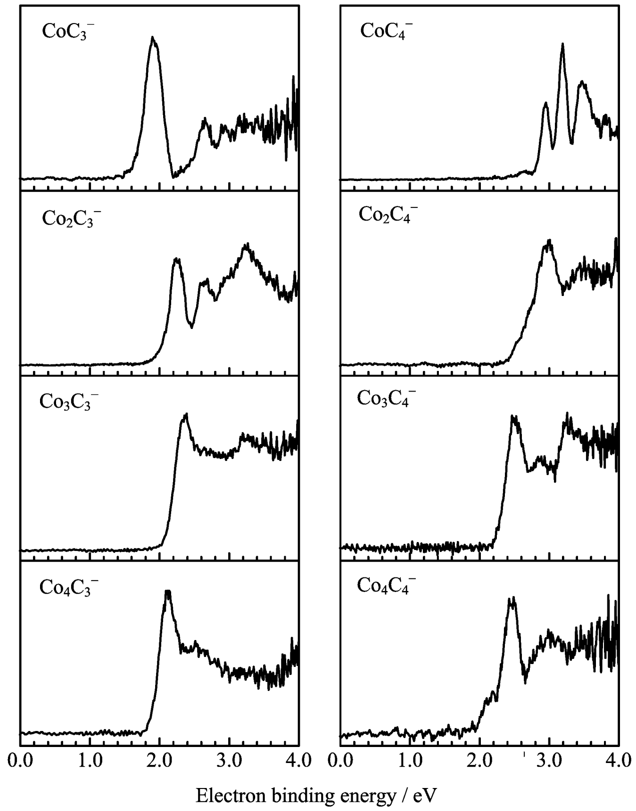

FIG. 2 Photoelectron spectra of $Co_nC_3^-$ and $Co_nC_4^-$ (n=1−4) clusters recorded with 266 nm photons.

III. RESULTS

A. Experimental results

A typical mass spectrum of cluster anions generated in our experiments is displayed in FIG. 1. In the mass spectrum, the highest intensity series is $Co_nC_3^-$ (n=1−4) and the second one is $Co_nC_4^-$ (n=1−4).

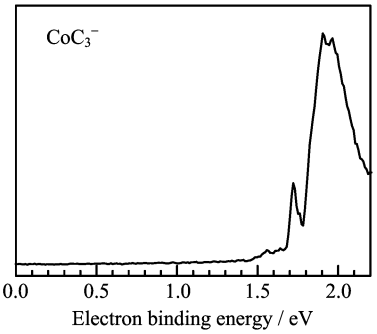

FIG. 3 Photoelectron spectrum of CoC_3^- recorded with 532 nm photons.

The photoelectron spectra of $Co_nC_3^-$ and $Co_nC_4^-$ (n=1−4) taken with 266 nm photons are presented in FIG. 2. The photoelectron spectrum of CoC_3^- taken with 532 nm photons is shown in FIG. 3. The VDEs and ADEs of these clusters estimated from the photoelectron spectra are listed in Table I. The VDE of each cluster was taken from the maximum of the first peak in its spectrum. The ADE of each cluster was determined by adding the value of instrumental resolution to the onset of the first peak in its spectrum. The onset of the first peak was determined by drawing a straight line along the leading edge of the first peak to cross the baseline of the spectrum.

1. $Co_nC_3^-$ (n=1−4)

The spectrum of CoC_3^- at 266 nm has a strong band centered at 1.90 eV, followed by two relatively weak bands centered at 2.65 and 2.94 eV. The strong band at 1.90 eV is resolved into two peaks centered at 1.72 and 1.93 eV in the 532 nm spectrum (FIG. 3). There is also a tail in the range of 1.46−1.66 eV in the 532 nm spectrum, which may be attributed to a hot band. The spectrum of $Co_2C_3^-$ shows three major bands centered at 2.24, 2.65, and 3.26 eV respectively. The third band at 3.26 eV is much broader than the other two bands. The 266 nm spectrum of $Co_2C_3^-$ in this work is consistent with the 355 nm spectrum reported by Tono *et al.* [42]. For the $Co_3C_3^-$ cluster, the spectrum has one resolved feature centered at 2.39 eV and another unresolved broad feature above 2.6 eV. With respect to $Co_4C_3^-$, its spectrum presents a sharp peak centered at 2.11 eV and some small peaks beyond 2.3 eV.

2. $Co_nC_4^-$ (n=1−4)

In the spectrum of CoC_4^-, there are five well resolved peaks centered at 2.64, 2.95, 3.19, 3.47, and 3.82 eV, respectively. The first peak at 2.64 eV is much weaker than the other peaks. $Co_2C_4^-$ shows a band centered at 2.99 eV, and followed by a broad feature in the range

DOI:10.1063/1674-0068/30/cjcp1710197

TABLE I Relative energies ΔE (in eV), theoretical VDEs and ADEs of the low-lying isomers of $Co_nC_3^-$ and $Co_nC_4^-$ (n=1−4) clusters, as well as the experimental VDEs and ADEs estimated from their photoelectron spectra.

Isomer	State	Sym.	ΔE	VDE/eV		ADE/eV		Isomer	State	Sym.	ΔE	VDE/eV		ADE/eV	
				Theo.	Expt.[a]	Theo.	Expt.[a]					Theo.	Expt.[a]	Theo.	Expt.[a]
CoC_3^- 1a	$^1A_1$	C_{2v}	0.00	1.81	1.72	1.79	1.67	CoC_4^- 1A	$^3\Sigma$	$C_{\infty v}$	0.00	2.64	2.64	2.58	2.48
1b	$^1\Sigma$	$C_{\infty v}$	0.21	1.81		1.71		1B	$^3A''$	C_s	0.14	2.86		2.43	
1c	$^3A_1$	C_{2v}	0.36	1.53		1.54		1C	$^3B_1$	C_{2v}	0.20	2.61		2.57	
$Co_2C_3^-$ 2a	$^4A_1$	C_{2v}	0.00	2.49	2.24	2.40	2.09	$Co_2C_4^-$ 2A	$^6A'$	C_s	0.00	2.90	2.99	2.82	2.57
2b	$^2A_2$	C_{2v}	0.268	2.24		2.13		2B	$^6B_2$	C_{2v}	0.06	2.76		2.70	
2c	$^2A'$	C_s	0.270	2.21		2.20		2C	^6A_g	C_{2h}	0.13	3.10		2.80	
$Co_3C_3^-$ 3a	$^5A'$	C_s	0.00	2.37	2.39	2.24	2.13	$Co_3C_4^-$ 3A	$^5B_2$	C_{2v}	0.00	2.08	2.46	2.06	2.26
3b	^7A	C_1	0.17	2.19		2.10		3B	^5A	C_2	0.01	2.17		2.07	
3c	^3A	C_1	0.18	2.26		2.27		3C	$^5A_2$	C_{2v}	0.15	2.19		1.89	
$Co_4C_3^-$ 4a	^8A	C_1	0.00	2.15	2.11	2.10	1.92	$Co_4C_4^-$ 4A	$^4A''$	C_s	0.00	2.37	2.47	2.14	2.21
4b	^8A	C_1	0.33	2.42		2.29		4B	$^2A''$	C_s	0.01	2.36		2.33	
4c	^6A	C_1	0.34	1.87		1.82		4C	$^6A'$	C_s	0.02	2.25	2.15	2.19	1.94

[a] The uncertainties of the experimental values are ±0.08 eV.

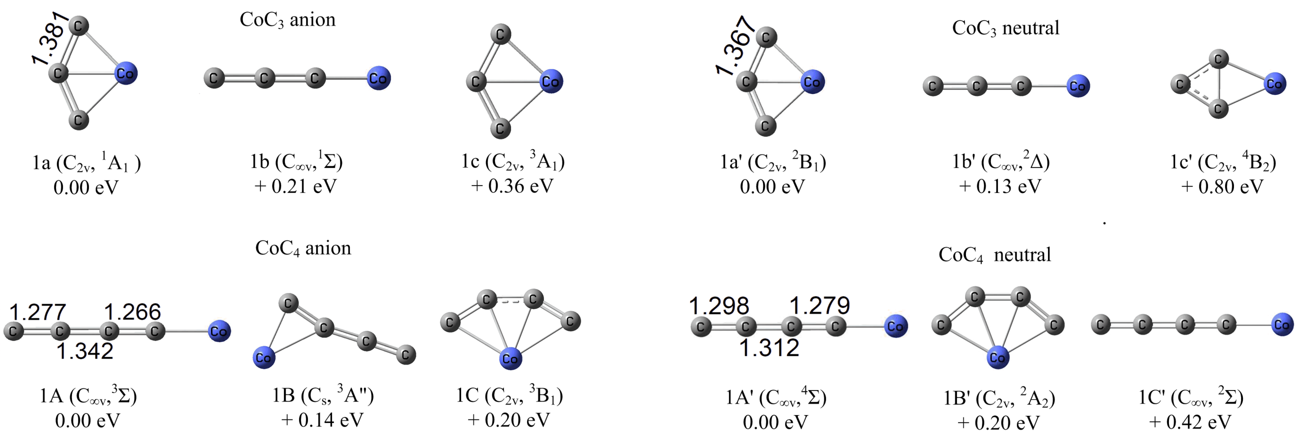

1a (C_{2v}, $^1A_1$) 0.00 eV; 1b ($C_{\infty v}$, $^1\Sigma$) + 0.21 eV; 1c (C_{2v}, $^3A_1$) + 0.36 eV; 1a' (C_{2v}, $^2B_1$) 0.00 eV; 1b' ($C_{\infty v}$, $^2\Delta$) + 0.13 eV; 1c' (C_{2v}, $^4B_2$) + 0.80 eV

1A ($C_{\infty v}$, $^3\Sigma$) 0.00 eV; 1B (C_s, $^3A''$) + 0.14 eV; 1C (C_{2v}, $^3B_1$) + 0.20 eV; 1A' ($C_{\infty v}$, $^4\Sigma$) 0.00 eV; 1B' (C_{2v}, $^2A_2$) + 0.20 eV; 1C' ($C_{\infty v}$, $^2\Sigma$) + 0.42 eV

FIG. 4 Geometries of the low-lying isomers of $CoC_3^{-/0}$ and $CoC_4^{-/0}$ optimized at the BPW91/6-311+G(d) level of theory. The bond lengths shown are in Å.

of 3.2−3.8 eV. The spectrum of $Co_3C_4^-$ displays three features centered at 2.46, 2.90, and 3.3 eV, respectively. The spectrum of $Co_4C_4^-$ exhibits a shoulder at 2.15 eV, followed by an intensive peak centered at 2.47 eV, and a broad band in the range of 2.7−3.3 eV.

B. Theoretical results

The typical low-lying isomers of $Co_nC_3^{-/0}$ and $Co_nC_4^{-/0}$ (n=1−4) are displayed in FIGs. 4−7 with the most stable structures on the left. More structures of these clusters can be found in the supplementary materials (FIGs. S1−S3). The symmetries, relative energies, and theoretical VDE and ADE values of $Co_nC_3^-$ and $Co_nC_4^-$ (n=1−4) are summarized in Table I along with the experimental VDE and ADE values for comparison. The Cartesian coordinates of the low-lying isomers of $Co_nC_3^-$ and $Co_nC_4^-$ (n=1−4) are available in the supplementary materials.

1. $CoC_3^{-/0}$ and $CoC_4^{-/0}$

The lowest-energy isomer of CoC_3^- (1a) is a fan-like structure with C_{2v} symmetry in $^1A_1$ electronic state. The theoretical VDE of isomer 1a is 1.81 eV, in agreement with the experimental measurement (1.72 eV). Isomer 1b is a C−C−C−Co linear structure in $^1\Sigma$ electronic state. Its energy is higher than isomer 1a by 0.21 eV. Isomer 1c is also a fan-like structure similar to that of isomer 1a, but it is in $^3A_1$ electronic state. It is much less stable in energy than isomer 1a by 0.36 eV. We suggest that isomer 1a is the most probable structure of CoC_3^- detected in our experiments. For neutral CoC_3, the most stable isomer 1a′ is also a fan-like structure in $^2B_1$ electronic state. Isomer 1b′ is

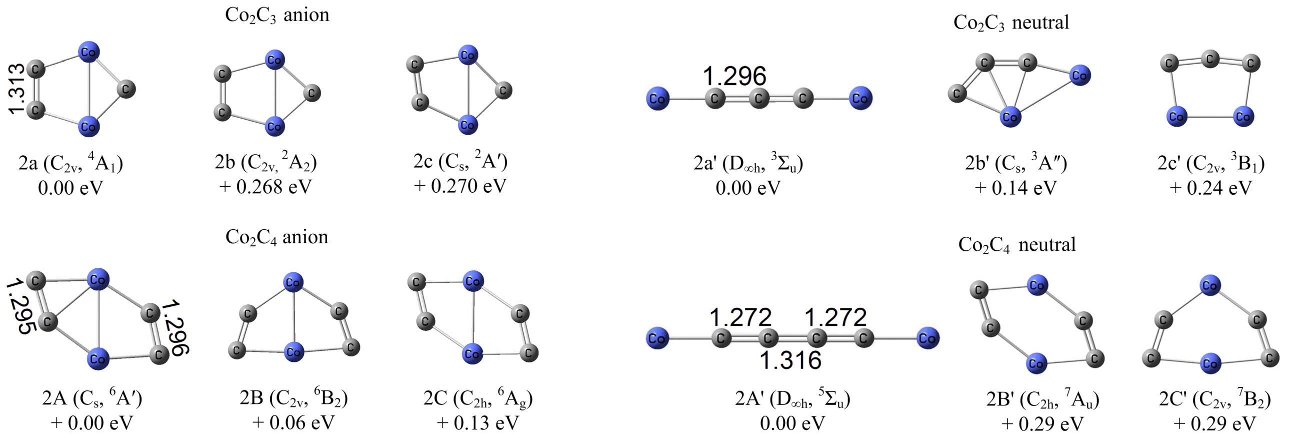

Co_2C_3 anion

2a (C_{2v}, $^4A_1$) 0.00 eV

2b (C_{2v}, $^2A_2$) + 0.268 eV

2c (C_s, $^2A'$) + 0.270 eV

Co_2C_3 neutral

2a' ($D_{\infty h}$, $^3\Sigma_u$) 0.00 eV

2b' (C_s, $^3A''$) + 0.14 eV

2c' (C_{2v}, $^3B_1$) + 0.24 eV

Co_2C_4 anion

2A (C_s, $^6A'$) + 0.00 eV

2B (C_{2v}, $^6B_2$) + 0.06 eV

2C (C_{2h}, ^6A_g) + 0.13 eV

Co_2C_4 neutral

2A' ($D_{\infty h}$, $^5\Sigma_u$) 0.00 eV

2B' (C_{2h}, ^7A_u) + 0.29 eV

2C' (C_{2v}, $^7B_2$) + 0.29 eV

FIG. 5 Geometries of the low-lying isomers of $Co_2C_3^{-/0}$ and $Co_2C_4^{-/0}$ optimized at the BPW91/6-311+G(d) level of theory. The bond lengths shown are in Å.

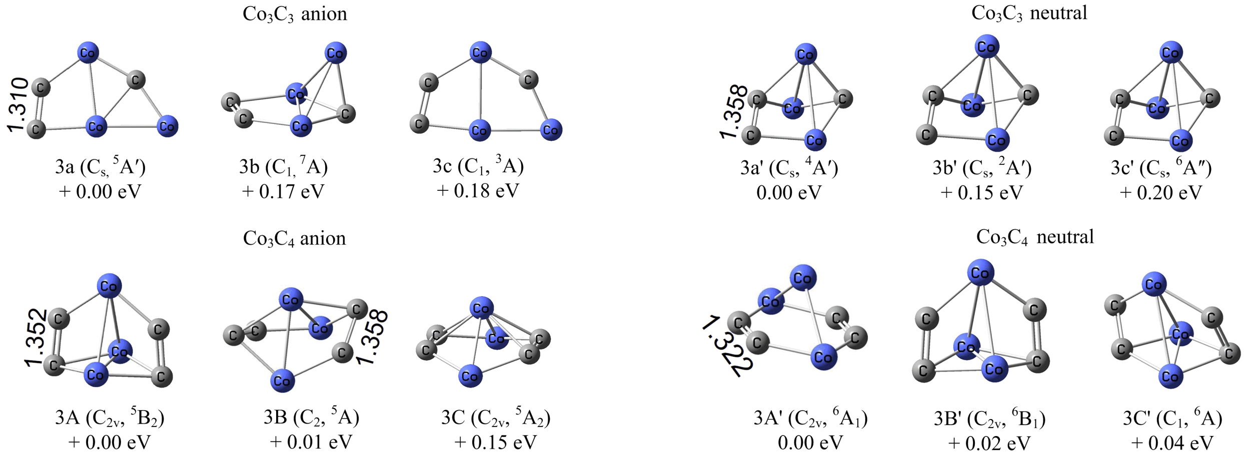

Co_3C_3 anion

3a (C_s, $^5A'$) + 0.00 eV

3b (C_1, ^7A) + 0.17 eV

3c (C_1, ^3A) + 0.18 eV

Co_3C_3 neutral

3a' (C_s, $^4A'$) 0.00 eV

3b' (C_s, $^2A'$) + 0.15 eV

3c' (C_s, $^6A''$) + 0.20 eV

Co_3C_4 anion

3A (C_{2v}, $^5B_2$) + 0.00 eV

3B (C_2, ^5A) + 0.01 eV

3C (C_{2v}, $^5A_2$) + 0.15 eV

Co_3C_4 neutral

3A' (C_{2v}, $^6A_1$) 0.00 eV

3B' (C_{2v}, $^6B_1$) + 0.02 eV

3C' (C_1, ^6A) + 0.04 eV

FIG. 6 Geometries of the low-lying isomers of $Co_3C_3^{-/0}$ and $Co_3C_4^{-/0}$ optimized at the BPW91/6-311+G(d) level of theory. The bond lengths shown are in Å.

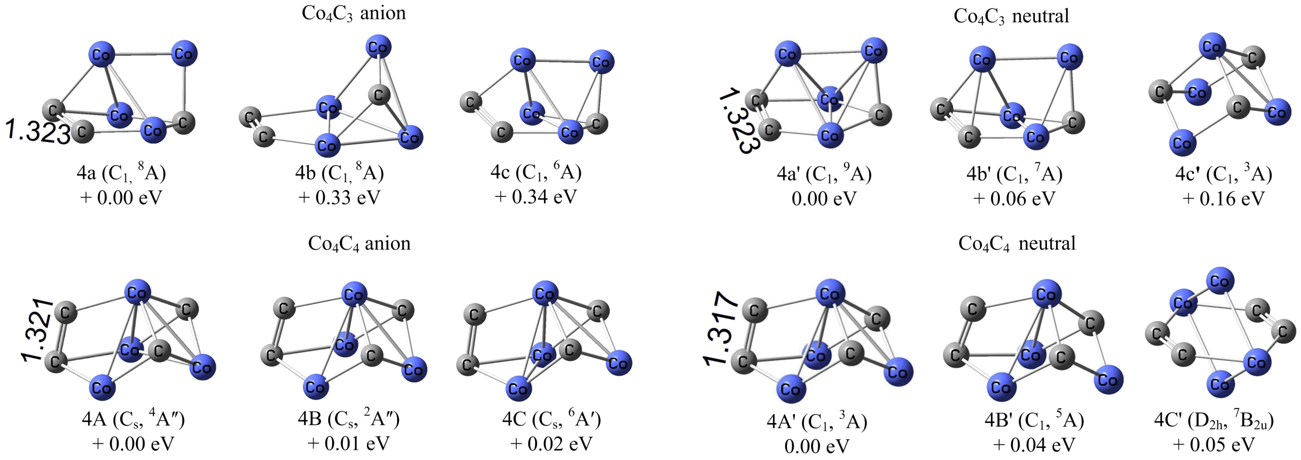

Co_4C_3 anion

4a (C_1, ^8A) + 0.00 eV

4b (C_1, ^8A) + 0.33 eV

4c (C_1, ^6A) + 0.34 eV

Co_4C_3 neutral

4a' (C_1, ^9A) 0.00 eV

4b' (C_1, ^7A) + 0.06 eV

4c' (C_1, ^3A) + 0.16 eV

Co_4C_4 anion

4A (C_s, $^4A''$) + 0.00 eV

4B (C_s, $^2A''$) + 0.01 eV

4C (C_s, $^6A'$) + 0.02 eV

Co_4C_4 neutral

4A' (C_1, ^3A) 0.00 eV

4B' (C_1, ^5A) + 0.04 eV

4C' (D_{2h}, $^7B_{2u}$) + 0.05 eV

FIG. 7 Geometries of the low-lying isomers of $Co_4C_3^{-/0}$ and $Co_4C_4^{-/0}$ optimized at the BPW91/6-311+G(d) level of theory. The bond lengths shown are in Å.

a C−C−C−Co linear structure in $^2\Delta$ electronic state. Isomer 1c′ consists of two isosceles triangles of C_3 and CoC_2 with a shared C−C bond. Isomers 1b′ and 1c′ are higher in energy than isomer 1a′ by 0.13 and 0.80 eV respectively.

Unlike the fan-like structure of CoC_3^-, the most stable structure of CoC_4^- (1A) is a $C_{\infty v}$ symmetric linear structure with the Co atom locating at one end of the C_4 chain. It is worth mentioning that the linear ground state structure of CoC_4^- anion is different from the fan-like structure of VC_4^- anion [18], but similar to the linear structure of CrC_4^- anion [60]. The structure of isomer 1B can be viewed as a Co atom binding to two C atoms of a C_4 carbon chain. Isomer 1C has a fan-like structure with the Co atom interacting with four C atoms of a C_4 chain. The theoretical VDE of isomer 1A is 2.64 eV, in excellent agreement with the experimental value (2.64 eV). Isomers 1B and 1C are higher in energy than isomer 1A by 0.14 and 0.20 eV, respectively. Therefore, we suggest isomer 1A to be the major species in our experiments, but the existence of isomer 1B cannot be ruled out. For neutral CoC_4, the most stable structure (1A′) has a linear structure with the Co atom locating at one end of the C_4 linear chain. Isomers 1B′ and 1C′ are higher in energy than isomer 1A′ by 0.20 and 0.42 eV. Isomer 1B′ is a fan-like structure. Isomer 1C′ has a linear structure similar to isomer 1A′. Isomer 1A′ is in quartet state while isomer 1C′ is in doublet state.

2. $Co_2C_3^{-/0}$ and $Co_2C_4^{-/0}$

The most stable isomer of $Co_2C_3^-$ (2a) is a C_{2v} symmetric planar structure with a Co−Co bond inserting between a C atom and a C_2 unit, which is similar to isomer A reported by Tono *et al.* [42]. The second and third isomers (2b and 2c) are similar to isomer 2a with their structures distorted slightly. Isomer 2a is in quartet state while isomers 2b and 2c are in doublet states. The theoretical VDE of isomer 2a (2.49 eV) is in reasonable agreement with the experimental value (2.24 eV). Isomers 2b and 2c are higher in energy than 2a by ∼0.27 eV. Isomer 2d (FIG. S1 in the supplementary materials) is a five-membereded ring with a C_3 chain, which is similar to isomer B calculated by Tono *et al.* [42]. The calculations of Tono *et al.* showed that isomers A and B are nearly degenerate with an energy difference of only 0.03 eV. In this work, isomer 2d is much less stable than isomer 2a by 0.35 eV. Therefore, we suggest that isomer 2a is the most probable structure of $Co_2C_3^-$. Different from the C_{2v} planar structure of $Co_2C_3^-$ anion, the most stable isomer of neutral Co_2C_3 (2a′) is a linear structure with two Co atoms locating at two ends of the C_3 chain, which is similar to the structure calculated by Ma *et al.* [37]. The second isomer of Co_2C_3 (2b′) can be viewed as adding a Co atom to the fan-like structure of CoC_3. The structure of isomer 2c′ is a five-membered ring formed by a C_3 chain and a Co_2 unit.

The most stable isomer of $Co_2C_4^-$ (2A) has a planar structure with two isolated C_2 units locating at two sides of the Co−Co bond. The structures of the second and third isomers (2B and 2C) are planar structures similar to 2A although they have different symmetries. Isomers 2B and 2C are higher in energy than isomer 2A by only 0.06 and 0.13 eV. The theoretical VDE of isomer 2A (2.90 eV) is consistent with the experimental measurement (2.99 eV), and that of isomer 2B (2.76 eV) is in accordance with the rising edge of the photoelectron spectrum of $Co_2C_4^-$. Thus, we suggest that isomers 2A and 2B may both be generated in our experiments, but the existence of isomer 2C cannot be ruled out. Interestingly, the most stable isomer of neutral Co_2C_4 (2A′) is a $D_{\infty h}$ symmetric linear structure, similar to the structure reported by Ma *et al.* [37], which is different from the planar structure of $Co_2C_4^-$ anion. The second and third isomers of neutral Co_2C_4 (2B′ and 2C′) are planar structures somewhat similar to those of $Co_2C_4^-$ anion.

3. $Co_3C_3^{-/0}$ and $Co_3C_4^{-/0}$

The three low-lying isomers of $Co_3C_3^-$ are derived by adding a Co atom to the planar structure of $Co_2C_3^-$. Isomers 3a and 3c are planar structures, while isomer 3b is a 3D structure in which a Co_3C tetrahedron interacts with a C_2 unit. The theoretical VDE of isomer 3a (2.37 eV) is in good agreement with the experimental value (2.39 eV). Although the calculated VDEs of isomers 3b and 3c are also close to the experimental measurement, they are higher in energy than 3a by 0.17 and 0.18 eV, respectively. Thus, we suggest that isomer 3a is the most likely structure for $Co_3C_3^-$. The low-lying isomers of neutral Co_3C_3 (3a′, 3b′, and 3c′) can be viewed as a Co_3 triangle inserting between a C atom and a C_2 unit.

The low-lying isomers of $Co_3C_4^-$ and Co_3C_4 all can be regarded as a Co_3 triangle inserting between two C_2 units although they have different C=C orientations as well as different bond lengths and bond angles. Isomers 3A and 3B are nearly degenerate in energy with 3B higher than 3A by only 0.01 eV. The low-lying isomers of neutral Co_3C_4 (3A′, 3B′, and 3C′) are also close in energy with the energy difference smaller than 0.04 eV. The calculated VDEs of isomers 3A (2.08 eV) and 3B (2.17 eV) are in reasonable agreement with the experimental value (2.46 eV). Isomer 3C is higher in energy than isomer 3A by 0.15 eV. Thus, we can infer that isomers 3A and 3B coexist in our experiments.

4. $Co_4C_3^{-/0}$ and $Co_4C_4^{-/0}$

The lowest-energy structure of anionic $Co_4C_3^-$ (isomer 4a) is composed of a C_2 unit and a C atom attaching to two faces of a Co_4 tetrahedron. The theoretical

DOI:10.1063/1674-0068/30/cjcp1710197

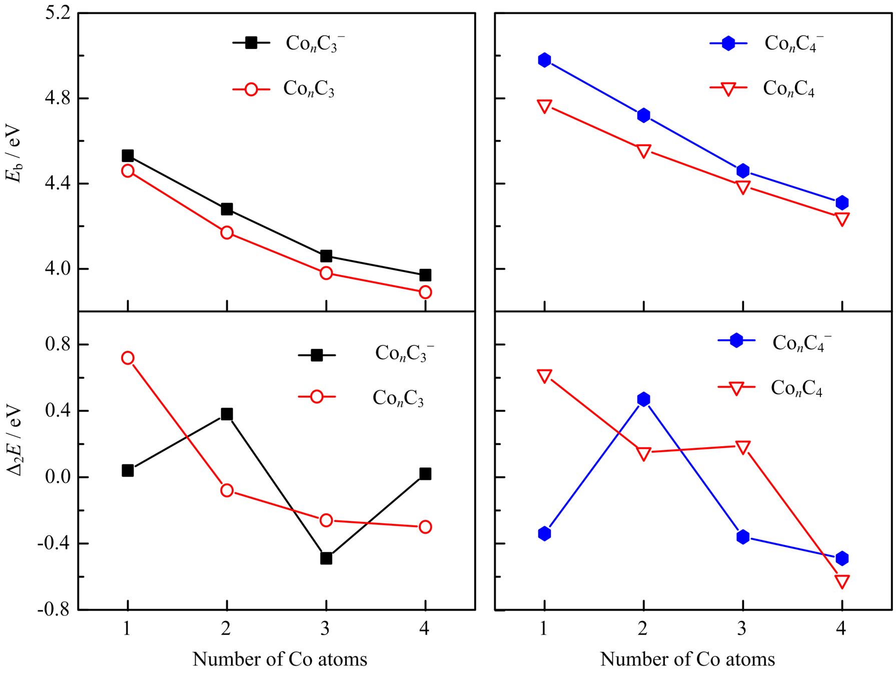

FIG. 8 Size dependence of binding energies (E_b) per atom and second-order energy difference (Δ_2E) for the most stable structures of $Co_nC_3{}^{-/0}$ and $Co_nC_4{}^{-/0}$ (n=1−4) clusters.

VDE of isomer 4a is 2.15 eV, in excellent agreement with the experimental measurement (2.11 eV). Isomers 4b and 4c are higher in energy than isomer 4a by 0.33 and 0.34 eV, respectively. Their VDEs deviate from the experimental value. Therefore, isomer 4a is the most probable one contributing to the experimental spectrum of $Co_4C_3{}^-$. For neutral Co_4C_3, the structures of isomers 4a′ and 4b′ are similar to that of isomer 4a, but they are in different electronic states. Isomer 4b′ is higher in energy than isomer 4a′ by only 0.06 eV. Isomer 4c′ is composed of a chair-like Co_3C_3 with alternating Co−C bond and an additional Co atom capping on the top of the chair-like Co_3C_3.

The low-lying isomers of $Co_4C_4{}^-$ (4A, 4B, and 4C) are all composed of a Co_4 tetrahedron adsorbing a C_2 unit and two C atoms on its three faces. They are nearly degenerate in energy, and have similar structures with different spin multiplicities. The theoretical VDEs of isomers 4A and 4B (2.37 and 2.36 eV) are all in agreement with the large peak (2.47 eV) and that of isomer 4C (2.25 eV) is consistent with the shoulder (2.15 eV). Therefore, we suggest that isomers 4A, 4B, and 4C may all be generated in our experiments. Similar to the structures of $Co_4C_4{}^-$ anion, the first two isomers of neutral Co_4C_4 (4A′ and 4B′) can also be viewed as a C_2 unit and two C atoms attaching to three faces of the Co_4 tetrahedron. Isomer 4C′ is an interesting D_{2h} symmetric structure with two parallel C_2 units locating at two sides of the long diagonal line of the Co_4 rhombus.

IV. DISCUSSION

Herein, we investigate the relative stabilities of $Co_nC_m{}^{-/0}$ clusters from their binding energies (E_b) per atom and second-order energy differences (Δ_2E). The E_b and Δ_2E of $Co_nC_m{}^{-/0}$ clusters are defined as follows:

$$E_b(Co_nC_m)=\frac{1}{n+m}[nE(Co)+mE(C)-E(Co_nC_m)] \quad (1)$$

$$E_b(Co_nC_m{}^-)=\frac{1}{n+m}[nE(Co)+(m-1)E(C)+E(C^-)-E(Co_nC_m{}^-)] \quad (2)$$

$$\Delta_2E(Co_nC_m{}^{-/0})=E(Co_{n-1}C_m{}^{-/0})+E(Co_{n+1}C_m{}^{-/0})-2E(Co_nC_m{}^{-/0}) \quad (3)$$

where E is the energy of the corresponding atom or cluster. The E_b and Δ_2E values of the most stable isomers of $Co_nC_3{}^{-/0}$ and $Co_nC_4{}^{-/0}$ versus n are plotted in FIG. 8. The E_b values of the anionic and neutral Co_nC_3 and Co_nC_4 clusters all decrease monotonously with increasing number of cobalt atoms. The E_b values of anionic Co_nC_3 and Co_nC_4 clusters are larger than those of their corresponding neutral counterparts, implying that an extra electron can strengthen the thermodynamic stabilities of these clusters. Moreover, the E_b values of $Co_nC_4{}^{-/0}$ are higher than those of the corresponding $Co_nC_3{}^{-/0}$. This suggests that carbon-rich $Co_nC_4{}^{-/0}$ clusters are more stable than carbon-deficient $Co_nC_3{}^{-/0}$ clusters. From FIG. 8, one can

DOI:10.1063/1674-0068/30/cjcp1710197

TABLE II ADCH charges on all carbon atoms (C^{charge}) and the highest C−C, Co−C, and Co−Co bond orders of the most stable isomers of $Co_nC_3^{-/0}$ and $Co_nC_4^{-/0}$ (n=1−4) clusters.

Neutral	C^{charge}/e	Wiberg bond order			Anion	C^{charge}/e	Wiberg bond order		
		C−C	Co−C	Co−Co			C−C	Co−C	Co−Co
CoC_3	−0.541	1.76	1.10	-	CoC_3^-	−1.018	1.77	1.27	-
Co_2C_3	−0.742	1.92	1.41	-	$Co_2C_3^-$	−0.909	2.26	1.50	0.70
Co_3C_3	−0.846	1.88	0.99	0.69	$Co_3C_3^-$	−0.864	2.26	1.28	1.22
Co_4C_3	−0.561	2.13	1.18	1.15	$Co_4C_3^-$	−0.706	2.17	1.15	1.15
CoC_4	−0.598	2.08	1.35	-	CoC_4^-	−0.962	2.34	1.17	-
Co_2C_4	−0.871	2.15	1.27	-	$Co_2C_4^-$	−1.148	2.41	0.86	1.14
Co_3C_4	−1.098	2.08	0.93	0.89	$Co_3C_4^-$	−1.086	1.95	0.92	0.51
Co_4C_4	−0.735	2.05	1.14	0.55	$Co_4C_4^-$	−0.958	2.09	1.16	0.51

find that the Δ_2E values of anionic $Co_nC_3^-$ have a strong odd-even oscillations with increasing number of cobalt atoms; however, those of neutral Co_nC_4 display an opposite weak oscillating trend. The Δ_2E values of anionic $Co_nC_4^-$ increase at n=2 and then continuously decrease at n=3, 4. $Co_2C_3^-$, $Co_2C_4^-$, and Co_3C_4 possess higher Δ_2E values than their adjacent clusters, indicating that they have higher stabilities than their neighboring sized clusters. For neutral Co_nC_3, the Δ_2E values decrease with increasing number of Co atoms, suggesting that smallest CoC_3 cluster is more stable than the larger sized clusters.

To understand the chemical bonding in $Co_nC_3^{-/0}$ and $Co_nC_4^{-/0}$ clusters, we conducted the atomic dipole corrected Hirshfeld (ADCH) population analysis and Wiberg bond order analysis, which are summarized in Table II. It is shown that the summed charges on the carbon units are negative for all anionic and neutral species, indicating that the electrons transfer from cobalt atoms to the carbon units. That is reasonable because the electronegativity of a C atom (2.55) is larger than that of a Co atom (1.88) [61]. The highest C−C bond orders of $Co_nC_3^{-/0}$ and $Co_nC_4^{-/0}$ are in the range of 1.76−2.34, suggesting the existence of C=C double bond in these clusters. The results are consistent with the calculated C−C bond lengths in $Co_nC_3^{-/0}$ and $Co_nC_4^{-/0}$ clusters, which are in the range of 1.266−1.381 Å, close to the C−C bond length in C_2H_4 molecule (1.339 Å) and larger than that in C_2H_2 molecule (1.203 Å). The Co−C bond orders are in the range of 0.86−1.50, indicating that the Co−C bonds in these clusters are mainly single bond.

It would be interesting to compare the structures of $Co_nC_4^{-/0}$ with those of $V_nC_4^{-/0}$ which have been investigated previously using photoelectron spectroscopy and DFT calculations by Yuan *et al.* [18]. The most stable structures of $VC_4^{-/0}$ are fan-like structures, whereas the geometries of $CoC_4^{-/0}$ are linear structures with the Co atom interacting with one end of the C_4 linear chain. Neutral Co_2C_4 has a $D_{\infty h}$ symmetric linear structure while neutral V_2C_4 has a three-dimensional structure with the carbon atom isolated by the V atoms into two perpendicular C_2 units. The ground state structures of $Co_2C_4^-$ and $Co_3C_4^{-/0}$ are similar to those of $V_2C_4^-$ and $V_3C_4^{-/0}$, which all have two isolated C_2 units connecting to the Co_n or V_n clusters. However, the lowest-energy structures of $Co_4C_4^{-/0}$ are very different from those of $V_4C_4^{-/0}$. In $Co_4C_4^{-/0}$, one C_2 unit and two C atoms interact with the Co_4 tetrahedron. In contrast, the four carbon atoms of $V_4C_4^{-/0}$ are completely isolated from each other by the V atoms. The structural differences between $Co_nC_4^{-/0}$ and $V_nC_4^{-/0}$ may arise from the different valence electrons of Co ($3d^74s^2$) and V ($3d^24s^2$) and different metal atom radius of Co (1.25 Å) and V (1.34 Å), which is in line with the results reported by von Helden *et al.* [62]. They suggested that metal carbides having a fcc crystal structure can be formed by carbon atoms intercalating into the octahedral holes of a regular metal lattice only when metal atom radius is above 1.3 Å. This structural disparity between $Co_nC_4^{-/0}$ and $V_nC_4^{-/0}$ reveals the different carbide-formation mechanisms between the early and the late 3d transition metals, which may also be one of the reasons that MXenes can be formed by the early transition metal carbides, rather than by the late transition metal carbides.

V. CONCLUSION

The structural and electronic properties of $Co_nC_3^{-/0}$ and $Co_nC_4^{-/0}$ (n=1−4) were investigated using anion photoelectron spectroscopy and DFT calculations. The adiabatic and vertical detachment energies of $Co_nC_3^-$ and $Co_nC_4^-$ were determined from their photoelectron spectra. The most stable structures of $Co_nC_3^{-/0}$ and $Co_nC_4^{-/0}$ were identified by comparing the calculated results and the experiment data. It is found that the $Co_2C_3^-$ and $Co_2C_4^-$ anions are planar structures, while the Co_2C_3 and Co_2C_4 neutrals are $D_{\infty h}$ symmetric linear structures, indicating the excess electron has an obvious influence on the structures of clusters. The structural evolution of $Co_nC_3^{-/0}$ and $Co_nC_4^{-/0}$ (n=1−4) indicates that the carbon atoms are sepa-

DOI:10.1063/1674-0068/30/cjcp1710197

rated gradually with increasing number of cobalt atoms although a C_2 unit remains at n=4. The average atomic binding energies of $Co_nC_3^{-/0}$ and $Co_nC_4^{-/0}$ (n=1−4) clusters decrease with increasing number of cobalt atoms and increase with increasing number of carbon atoms. The ADCH charge distributions on carbon atoms indicate that the electrons transfer from cobalt atoms to the carbon units.

Supplementary materials: The relative energies and vertical detachment energies of $Co_{1,2}C_3^-$ calculated from different basis set, more structures of $Co_nC_3^{-/0}$ and $Co_nC_4^{-/0}$ (n=2−4) clusters, and Cartesian coordinates of $Co_nC_3^-$ and $Co_nC_4^-$ (n=1−4) clusters.

VI. ACKNOWLEDGEMENTS

This work was supported by the National Natural Science Foundation of China (No.21303214), Jin-yun Yuan acknowledges the National Natural Science Foundation of China (No.21401064) and the Open research fund of Beijing National Laboratory for Molecular Sciences (No.20140164) for financial support. The theoretical calculations were conducted on the China Scientific Computing Grid (ScGrid).

[1] R. B. Levy and M. Boudart, Science **181**, 547 (1973).
[2] J. G. G. Chen, Chem. Rev. **96**, 1477 (1996).
[3] H. F. Li, Y. X. Zhao, Z. Yuan, Q. Y. Liu, Z. Y. Li, X. N. Li, C. G. Ning, and S. G. He, J. Phys. Chem. Lett. **8**, 605 (2017).
[4] Y. Chai, T. Guo, C. M. Jin, R. E. Haufler, L. P. F. Chibante, J. Fure, L. H. Wang, J. M. Alford, and R. E. Smalley, J. Phys. Chem. **95**, 7564 (1991).
[5] D. E. Clemmer, K. B. Shelimov, and M. F. Jarrold, Nature **367**, 718 (1994).
[6] D. E. Clemmer, J. M. Hunter, K. B. Shelimov, and M. F. Jarrold, Nature **372**, 248 (1994).
[7] B. C. Guo, K. P. Kerns, and A. W. Castleman Jr., Science **255**, 1411 (1992).
[8] B. C. Guo, S. Wei, J. Purnell, S. Buzza, and A. W. Castleman Jr., Science **256**, 515 (1992).
[9] J. S. Pilgrim and M. A. Duncan, J. Am. Chem. Soc. **115**, 6958 (1993).
[10] S. Li, H. B. Wu, and L. S. Wang, J. Am. Chem. Soc. **119**, 7417 (1997).
[11] M. Naguib, M. Kurtoglu, V. Presser, J. Lu, J. J. Niu, M. Heon, L. Hultman, Y. Gogotsi, and M. W. Barsoum, Adv. Mater. **23**, 4248 (2011).
[12] M. Naguib, J. Come, B. Dyatkin, V. Presser, P. L. Taberna, P. Simon, M. W. Barsoum, and Y. Gogotsi, Electrochem. Commun. **16**, 61 (2012).
[13] Y. Zhong, X. H. Xia, F. Shi, J. Y. Zhan, J. P. Tu, and H. J. Fan, Adv. Sci. (Weinh) **3**, 1500286 (2016).
[14] P. Nikolaev, M. J. Bronikowski, R. K. Bradley, F. Rohmund, D. T. Colbert, K. A. Smith, and R. E. Smalley, Chem. Phys. Lett. **313**, 91 (1999).
[15] D. S. Bethune, C. H. Klang, M. S. de Vries, G. Gorman, R. Savoy, J. Vazquez, and R. Beyers, Nature **363**, 605 (1993).
[16] W. H. Chiang and R. M. Sankaran, Nature Mater. **8**, 882 (2009).
[17] F. Yang, X. Wang, D. Q. Zhang, J. Yang, D. Luo, Z. W. Xu, J. K. Wei, J. Q. Wang, Z. Xu, F. Peng, X. M. Li, R. M. Li, Y. L. Li, M. H. Li, X. D. Bai, F. Ding, and Y. Li, Nature **510**, 522 (2014).
[18] J. Y. Yuan, P. Wang, G. L. Hou, G. Feng, W. J. Zhang, X. L. Xu, H. G. Xu, J. L. Yang, and W. J. Zheng, J. Phys. Chem. A **120**, 1520 (2016).
[19] A. B. C. Patzer, C. Chang, and D. Sülzle, Chem. Phys. Lett. **612**, 39 (2014).
[20] X. B. Wang, C. F. Ding, and L. S. Wang, J. Phys. Chem. A **101**, 7699 (1997).
[21] J. W. Fan, L. Lou, and L. S. Wang, J. Chem. Phys. **102**, 2701 (1995).
[22] J. W. Fan and L. S. Wang, J. Phys. Chem. **98**, 11814 (1994).
[23] H. J. Zhai, S. R. Liu, X. Li, and L. S. Wang, J. Chem. Phys. **115**, 5170 (2001).
[24] K. L. Knappenberger Jr., P. A. Clayborne, J. U. Reveles, M. A. Sobhy, C. E. Jones Jr., U. U. Gupta, S. N. Khanna, I. Iordanov, J. Sofo, and A. W. Castleman Jr., ACS Nano **1**, 319 (2007).
[25] M. A. Brewster and L. M. Ziurys, Astrophys. J. **559**, L163 (2001).
[26] R. J. van Zee, J. J. Bianchini, and W. Weltner Jr., Chem. Phys. Lett. **127**, 314 (1986).
[27] A. G. Adam and J. R. D. Peers, J. Mol. Spectrosc. **181**, 24 (1997).
[28] M. Barnes, A. J. Merer, and G. F. Metha, J. Chem. Phys. **103**, 8360 (1995).
[29] J. R. Guo, Z. X. Zhang, T. T. Wang, C. X. Chen, and Y. Cheng, Chin. J. Chem. Phys. **21**, 505 (2008).
[30] H. Huang, Y. C. Chang, Z. H. Luo, X. Y. Shi, C. S. Lam, K. C. Lau, and C. Y. Ng, J. Chem. Phys. **138**, 094301 (2013).
[31] A. C. Borin, J. P. Gobbo, and B. O. Roos, Chem. Phys. Lett. **418**, 311 (2006).
[32] G. L. Gutsev, L. Andrews, and C. W. Bauschlicher Jr., Theor. Chem. Acc. **109**, 298 (2003).
[33] D. Tzeli and A. Mavridis, J. Phys. Chem. A **110**, 8952 (2006).
[34] K. C. Lau, Y. Pan, C. S. Lam, H. Huang, Y. C. Chang, Z. H. Luo, X. Y. Shi, and C. Y. Ng, J. Chem. Phys. **138**, 094302 (2013).
[35] P. Redondo, C. Barrientos, and A. Largo, Int. J. Quantum Chem. **108**, 1684 (2008).
[36] P. Redondo, C. Barrientos, and A. Largo, Int. J. Mass Spectrom. **272**, 187 (2008).
[37] Q. M. Ma, Y. Liu, Z. Xie, and J. Wang, J. Nanosci. Nanotechnol. **10**, 5490 (2010).
[38] Z. H. Chen and Z. Xie, Eur. Phys. J. Appl. Phys. **67**, 10403 (2014).
[39] B. Zhang, B. B. Cao, C. Chen, J. Zhang, and H. M. Duan, J. Clust. Sci. **24**, 197 (2013).
[40] X. Li and L. S. Wang, J. Chem. Phys. **111**, 8389 (1999).
[41] L. S. Wang and X. Li, J. Chem. Phys. **112**, 3602 (2000).
[42] K. Tono, A. Terasaki, T. Ohta, and T. Kondow, J. Chem. Phys. **117**, 7010 (2002).
[43] J. Y. Yuan, H. G. Xu, and W. J. Zheng, Phys. Chem.

Chem. Phys. **16**, 5434 (2014).

[44] J. Y. Yuan, G. L. Hou, B. Yang, H. G. Xu, and W. J. Zheng, J. Phys. Chem. A **118**, 6757 (2014).

[45] J. Y. Yuan, H. G. Xu, Z. G. Zhang, Y. Feng, and W. J. Zheng, J. Phys. Chem. A **115**, 182 (2011).

[46] J. M. Xiong, Y. J. Ding, T. Wang, L. Yan, W. M. Chen, H. J. Zhu, and Y. Lu, Catal. Lett. **102**, 265 (2005).

[47] V. G. Harris, Y. Chen, A. Yang, S. Yoon, Z. Chen, A. Geiler, C. Chinnasamy, L. H. Lewis, C. Vittoria, E. E. Carpenter, K. J. Carroll, R. Goswami, M. A. Willard, L. Kurihara, M. Gjoka, and O. Kalogirou, J. Phys. D **43**, 165003 (2010).

[48] P. Gao, Y. Wang, S. Q. Yang, Y. J. Chen, Z. Xue, L. Q. Wang, G. B. Li, and Y. Z. Sun, Int. J. Hydrogen Energ. **37**, 17126 (2012).

[49] H. G. Xu, Z. G. Zhang, Y. Feng, J. Y. Yuan, Y. C. Zhao, and W. J. Zheng, Chem. Phys. Lett. **487**, 204 (2010).

[50] J. Lv, Y. C. Wang, L. Zhu, and Y. M. Ma, J. Chem. Phys. **137**, 084104 (2012).

[51] A. D. Becke, Phys. Rev. A **38**, 3098 (1988).

[52] J. P. Perdrew and Y. Wang, Phys. Rev. B **45**, 13244 (1992).

[53] M. J. Frisch, G. W. Trucks, H. B. Schlegel, G. E. Scuseria, M. A. Robb, J. R. Cheeseman, G. Scalmani, V. Barone, B. Mennucci, G. A. Petersson, H. Nakatsuji, M. Caricato, X. Li, H. P. Hratchian, A. F. Izmaylov, J. Bloino, G. Zheng, J. L. Sonnenberg, M. Hada, M. Ehara, K. Toyota, R. Fukuda, J. Hasegawa, M. Ishida, T. Nakajima, Y. Honda, O. Kitao, H. Nakai, T. Vreven, J. A. Montgomery, Jr., J. E. Peralta, F. Ogliaro, M. Bearpark, J. J. Heyd, E. Brothers, K. N. Kudin, V. N. Staroverov, R. Kobayashi, J. Normand, K. Raghavachari, A. Rendell, J. C. Burant, S. S. Iyengar, J. Tomasi, M. Cossi, N. Rega, J. M. Millam, M. Klene, J. E. Knox, J. B. Cross, V. Bakken, C. Adamo, J. Jaramillo, R. Gomperts, R. E. Stratmann, O. Yazyev, A. J. Austin, R. Cammi, C. Pomelli, J. W. Ochterski, R. L. Martin, K. Morokuma, V. G. Zakrzewski, G. A. Voth, P. Salvador, J. J. Dannenberg, S. Dapprich, A. D. Daniels, O. Farkas, J. B. Foresman, J. V. Ortiz, J. Cioslowski, and D. J. Fox, *Gaussian 09, Revision A.02*, Wallingford CT: Gaussian, Inc. (2009).

[54] R. Z. Li, H. G. Xu, X. L. Xu, and W. J. Zheng, Chem. Phys. Lett. **607**, 105 (2014).

[55] T. H. Dunning Jr., J. Chem. Phys. **90**, 1007 (1989).

[56] T. Lu and F. W. Chen, J. Theor. Comput. Chem. **11**, 163 (2012).

[57] T. Lu and F. W. Chen, J. Comp. Chem. **33**, 580 (2012).

[58] T. Lu and F. W. Chen, Acta Phys. Chim. Sin. **28**, 1 (2012).

[59] A. E. Reed, L. A. Curtiss, and F. Weinhold, Chem. Rev. **88**, 899 (1988).

[60] H. J. Zhai, L. S. Wang, P. Jena, G. L. Gutsev, and C. W. Bauschlicher Jr., J. Chem. Phys. **120**, 8996 (2004).

[61] L. Pauling, *The Nature of the Chemical Bond*, 3rd Edn., Ithaca, New York: Cornell University Press, (1960).

[62] G. von Helden, D. van Heijnsbergen, and G. Meijer, J. Phys. Chem. A **107**, 1671 (2003).

DOI:10.1063/1674-0068/30/cjcp1710197